

All the Feels: A dexterous hand with large area sensing

Raunaq Bhirangi^{†,1,2}, Abigail DeFranco^{*,1}, Jacob Adkins^{*,1}, Carmel Majidi¹, Abhinav Gupta¹,
Tess Hellebrekers² and Vikash Kumar^{†,2}

Abstract—High cost and lack of reliability has precluded the widespread adoption of dexterous hands in robotics. Furthermore, the lack of a viable tactile sensor capable of sensing over the entire area of the hand impedes the rich, low-level feedback that would improve learning of dexterous manipulation skills. This paper introduces an inexpensive, modular, robust, and scalable platform - the *D'Manus* - aimed at resolving these challenges while satisfying the large-scale data collection capabilities demanded by deep robot learning paradigms. Studies on human manipulation point to the criticality of low-level tactile feedback in performing everyday dexterous tasks. The *D'Manus* comes with ReSkin sensing on the entire surface of the palm as well as the fingertips. We demonstrate effectiveness of the fully integrated system in a tactile aware task - bin picking and sorting. Code, documentation, design files, detailed assembly instructions, trained models, task videos, and all supplementary materials required to recreate the setup can be found on <http://roboticsbenchmarks.org/platforms/dmanus>

I. INTRODUCTION

As humans, we routinely operate in unstructured, cluttered environments through a series of imprecise, improvised motions. Think about finding the keys hiding at the bottom of your bag, pulling a box from the back of the fridge or finding the steel ladle among the wooden spatulas. While we rely on vision for these tasks to plan motion at a high level, executing each of these motions involves using low-level tactile signals to understand the environment and characterize the objects we touch along the way so as to effectively leverage the dexterity of the human hand. In moving towards endowing robots with this ability, we present a fully sensorized prehensile hand with the sensory capabilities to feel around and distinguish objects in a cluttered environment.

As data-driven methods have gathered momentum for robot learning in the real world [1], [2], [3], success with dexterous manipulators has been limited and often restricted to simulation [4], [5]. While dexterous hands are inherently difficult to control due to the large number of degrees of freedom (DoF) as well as the contact-rich nature of the tasks involved, their high cost [6] and lack of reliability is fundamentally incompatible with the large-scale data collection needs of modern-day deep learning. Efforts aimed at developing reliable hardware that can withstand the data demands of real-world robot learning have been few and far in between [7], [8]. As a result, dexterous learning in the real world has been limited to the few groups that have access to the significant cost and resources involved [9].

*equal contribution

[†]Correspondence: rbhirang@cs.cmu.edu, vikashplus@gmail.com

¹Carnegie Mellon University

²FAIR-MetaAI



Fig. 1: The *D'Manus* – a low-cost, 10 DoF, reliable prehensile hand with all-over ReSkin [12] sensing

Closed loop dexterous control in contact-rich tasks is made even more difficult by the absence of integrated tactile sensing that can provide rich sensory feedback over the surface of the hand. Despite the promise of robot learning from vision, the complexity of dexterous control in occluded environments has precluded learning visuomotor policies in the real world. The occasional success stories [9], while impressive, get around the occlusions by using a large number of cameras that would be impractical outside a laboratory setting. As robots move towards being deployed in homes and other unstructured environments, it becomes increasingly critical for them to be adept at handling the ubiquitous occluded settings that humans operate in. While the importance of all-over sensing, especially over the palm, has been well-studied in the context of human dexterity [10], most existing dexterous robotic hands either lack tactile sensing altogether [11], or focus primarily on fingertip sensing.

To counter these challenges, we present the *D'Manus* – an inexpensive, robust prehensile hand that is built to withstand the vagaries of real-world robot learning. We use ReSkin [13], [12] to successfully integrate large area tactile sensing for a fully sensorized palm and fingertips. We exhibit the system's effectiveness and strengths by learning tactile models for object identification as well as category-

level softness and texture identification. Furthermore, we demonstrate generalization of our learned models to unseen objects and environments by validating their performance in a highly tactile-aware task – bin sorting.

II. RELATED WORK

A. Data-driven methods and dexterous manipulation

Dexterous manipulation evolves in a compact space which is inhibited by the static (joint limits) and dynamic constraints (intermittent contact with objects, self collisions, slip) from the hand as well as the object’s DoFs. Classical methods [14], [15], [16] that explicitly reason over the entire space struggle to scale due to the curse of dimensionality. The rise of deep learning and its promised potential for handling large action spaces has prompted a number of recent works aimed at solving dexterous manipulation using deep neural networks [17], [18], [9], [19]. Conspicuously, most of these methods use a single exteroceptive sensory modality – vision [20], [9]. While vision provides rich sensory information about the scene and the visual properties of objects, and has been successfully used in robot learning [1], [2], [21], [3], dexterous tasks are generally contact-rich and require reasoning about contact information that cannot be captured entirely using vision. We posit that the lack of rich tactile information limits a manipulator’s ability to effectively perform real-world dexterous manipulation tasks involving force control, flexible objects, and deformable media (dough making), particularly with smaller objects which receive degraded visual signals due to occlusions.

Additionally, if we look to humans for inspiration, it is apparent that our end-effectors (hands) have all-over sensing, which is imperative to our ability to effectively perform contact-rich manipulation tasks [10]. This points to a need for a similar sensing modality in robotic end effectors that can capture local contact characteristics over the possible contact areas of the hand. There has been some recent work in adding MEMS sensors [22], audio [23], contact microphones [24], [25] and optical tactile sensors [26], [27] as additional modalities to vision for robot learning. However, their constraints on form factor have restricted these sensors to parallel jaw grippers. With this work, we present a low-cost, reliable dexterous platform with integrated large area sensing that offers a rich tactile sensory modality with large spatial coverage suitable for contact-rich manipulation.

B. Robot hands

The versatility of the human hand has long inspired a number of efforts aimed at creating similarly capable robotic hands dating back to the early days of robotics [28], [29], [30], [31]. Concurrent work in prosthetics and assistive robotics [32], [33], [34] has often overlapped with and contributed to research in creating general-purpose robotic hands. More recently, advances in material science and rapid prototyping as well as control algorithms have further pushed the envelope of capable dexterous hands [35]. Since these efforts have primarily been directed towards demonstrating added functionality on human control, they tend to fall short

on the scalability, reliability, affordability, and other capabilities required for prolonged operation in unstructured settings. Despite the recent advancements in data-driven robotics [1], [2], robust platforms capable of meeting the data needs of real-world learning have been few and far in between [7], [19], [36]. This has restricted recent investigations with dexterous hands to simulation [4], [5] or the few researchers who can afford the hardware expense [9].

Beyond reliability, most dexterous hands entirely lack or possess limited tactile sensing [11]. Discovery of contact rich dexterous behaviors, difficult due to the high DoF, is further complicated by a lack of critical contact information from extrinsic tactile sensing. Most attempts at adding tactile sensors to robot hands have been restricted to fingertip sensing [37], [38], [39], [40], [41]. Moreover, these solutions tend to be bulky [37], difficult to fabricate and replace [38], [39], [37], [42], and/or further add to the cost of the already expensive hand [43]. In contrast, we present *D’Manus*– a robust low cost prehensile hand capable of meeting the sensing [13], [12] and robustness [7] needs of data driven methods. To the best of our knowledge, we present the first sensorized hand with full tactile sensing on the palm, which has been shown to be critical to human dexterous ability [44], [45].

C. Tactile sensing

Tactile sensing has a long history in robotic grasping and manipulation [46]. A number of different modalities like capacitive [47], [48], [42], resistive [37], piezoelectric [39] and MEMS [38]-based sensors have been explored as tactile sensing alternatives for robotics. With the recent success of deep learning, especially in computer vision, optical tactile sensors [49], [50] have emerged as the popular choice of tactile sensor, due to their high resolution as well as their compatibility with neural architectures for processing signals. Most of these solutions however are either bulky [49], [50], difficult to fabricate [47], [48], [37] or lack shear sensing capabilities. Further, a number of sensors need direct electrical connections between the circuitry and the interface [38], [39], [37] and cannot be easily replaced – an important consideration for large-scale data collection given the inevitable wear-and-tear that comes from soft-hard interfaces. Moreover, a number of these sensors do not scale to larger spatial coverage which is critical to capturing contact characteristics for contact-rich dexterous manipulation tasks. Some recent attempts that have been more successful at creating sensing skins with large area coverage include the MIT Glove [51], hex-o-skin [42], [52] among others [47], [48], [53]. None of these works however, demonstrate the use of these large-area sensing capabilities in a robot learning setting. In this paper, we build on ReSkin [13], [12], a magnetic elastomer-based tactile sensor that avoids these pitfalls. The variable form factor and versatility of the sensor enables us to scale it up to the entire area of the palm as well as the fingertips while preserving the sharp fingertips/nails that imperative to dexterous manipulation [44], [45].

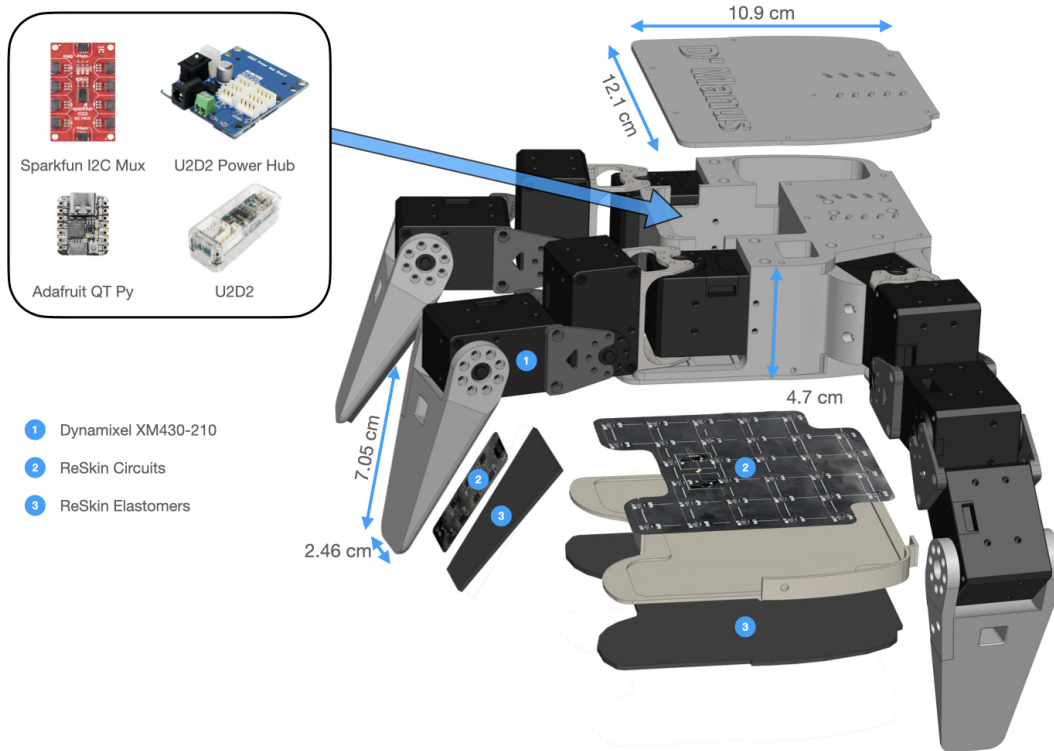


Fig. 2: **Anatomy of the *D'Manus* hand:** The hand is actuated at joint level using Dynamixel XM430-210 smart actuators. ReSkin sensors are integrated with the fingertips and the palm. Each fingertip sensor is comprised of 8 magnetometers while the palm sensor consists of 32 magnetometers for a total of 56 magnetometers. Sensor and motor interfacing components are housed in the core of the hand.

III. PLATFORM AND SYSTEM DETAILS

The *D'Manus* is a low-cost, reliable prehensile robotic hand with immersive tactile sensing over its larger contact surfaces, i.e. the palm and fingertips. To the benefit of the community and facilitate adoption, *D'Manus* is released as an open-sourced manipulation platform¹. In this section, we detail the features and properties of the system.

A. The Hand: Construction and Interfacing

The *D'Manus* hand is a three-fingered, 10-DoF hand – each finger has three degrees of freedom, with a fourth DoF for the thumb. The hand is actuated at joint-level via Dynamixel smart actuators. A 12V power supply is used to power the hand and a USB-serial bus is used for communication between the hand and a control computer. Non-actuated elements of the hand like the palm and the fingertips are 3D printed and the actuators are daisy chained. This allows the *D'Manus* to be easily customized and assembled while maintaining a low price point (\$4000). The hand can be made compatible to be mounted on any robot arm or wrist attachment of choice using a simple 3D printed adaptor. While we experimented with versions of the platform with up to 16 DoFs, we converged on the 10 DoF *D'Manus* as it strikes a balance between dexterity, cost, robustness, weight, and size.

¹CAD models, bill of materials, circuit designs, assembly and setup instructions, we can be found on <http://roboticsbenchmarks.org/platforms/dmanus>

B. Large-area Exteroceptive Sensing: ReSkin

We use ReSkin [13], [12] to endow the hand with large-area exteroceptive tactile sensing. ReSkin uses a magnetic elastomer interface with magnetometer circuits underneath to detect deformation. Drawing from [12], we scale the sensor circuits and the skins to the size of the palm and the fingertips while maintaining a thickness of 2mm for the skins. The magnetic elastomers are similarly scaled to the size of the fingertips and the palm with a change in their magnetization procedure – the skins are allowed to cure at room temperature without interfering magnetic fields and then magnetized using a pulse magnetizer with a 4 Tesla (40 kOe) impulse. This change is motivated by two factors: (a) a stronger magnetic field (2-3x) for the same deformation, and (b) ease and scalability of fabrication by eliminating individual molds made of magnets that scale poorly with the size of the skin. Data from the sensors is streamed to the control computer via USB through a microcontroller + I2C mux.

Property	Options
Control	Position, Velocity, Extended Position, Current, PWM
Proprioceptive Sensing	Position, Velocity, Current, Realtime tick, Trajectory, Input Voltage
Exteroceptive Sensing	ReSkin (30 Hz)
Limits	Position, Velocity, PWM, Current
Baudrate	9600 bps ~ 4.5 Mbps

TABLE I: Operational Details for the *D'Manus*

C. Proprioceptive Sensing, Control and Reliability

The use of Dynamixel smart actuators affords the *D’Manus* a range of control modes as well as proprioceptive sensing capabilities as outlined in Table I. In terms of reliability, amongst various versions of the platform we have over 10,000 hours of operational time over the course of 12 months in 3 different locations with a total of 5 breakages. These consisted of three motor failures, one 3D printed part failure, and operational deterioration of wires – all of which were repaired in-house within 30 minutes by non expert users. The version of the platform being release has significantly benefited from aggressive real world testing of prior versions. The specific copy of the *D’Manus* we are presenting results on has been used for over 400 hours over the last 8 months with no breakages.

D. Software

D’Manus comes with a python driver that exposes all operational modalities outlined in Table I. We also developed a detailed simulation model of the *D’Manus* based on MuJoCo (Figure 3) that features a data-driven approximate model of ReSkin sensors intended for experimental prototyping.



Fig. 3: Simulated *D’Manus*

IV. EXPERIMENTAL SETUP AND DESIGN

To further explicate the capabilities of the proposed *D’Manus*, we provide three sets of experiments. First, we study the dexterity of the prehensile hand in grasping a diverse set of objects. Next, to validate our emphasis on large area tactile sensing, we start with a controlled experiment investigating the ability of the *D’Manus* to perform object identification based on tactile properties agnostic to shape and size characteristics. We follow this up with a study on generalization of such tactile associations to unseen objects by learning models for category-level identification of softness and textures. Finally, we corroborate the generalizability of our identification models to unseen real world interactions by deploying the *D’Manus* in a tactile-rich binning setup and demonstrating automated bin sorting purely from tactile information (no visual inputs). In the remainder of this section, we elaborate on the hardware setup and the data collection procedure used for the tactile sensing validation experiments.

A. Hardware setup

While *D’Manus* can be mounted on any robot arm of choice using a 3D printed attachment, we use a Franka Emika Panda robot (integrated using the `polymetis` drivers [54]) for all our experiments.

B. Data Collection

For ease of collecting tactile interaction data, we fix the palm in an upright position as shown in Fig. 4. To collect a trajectory of interaction data for an object, it is individually placed on the palm and a human scripted policy (30 Hz) for motor babbling is executed to gather data for 10 seconds. Each frame in the trajectory consists of tactile signals (3-axis magnetic flux measurements for each of the 56 magnetometers concatenated into a 168-dimensional signal) and the corresponding object label. These object labels are used to assign a category label for each frame during training and inference depending on the task in question.



Fig. 4: **Data collection setup:** Tactile data is collected by placing the object on the palm and executing a human-scripted interaction policy for motor babble.

C. Model Architecture

For all our learning experiments, we examine two neural architectures: a fully-connected architecture (MLP) and a recurrent architecture (RNN) which consists of an LSTM followed by fully connected layers. Each frame of tactile data from ReSkin consists of a 168-dimensional magnetic flux vector. The use of a recurrent architecture is an attempt to leverage the temporally correlated nature of streamed tactile data. We sequentially feed in single frames of data from the entire trajectory and make predictions at every timestep. In the same vein, to provide the MLP networks with temporal information, we input stacked frames of ReSkin data to the network. For each of our experiments, we sweep over different parameters for the MLP – frame-stack size, frames skipped between stacked frames, hidden layer size, number of hidden layers – and the RNN – LSTM parameters (layer size, number of layers), fully connected layers (layer sizes, number of layers). Results presented in the following section correspond to the best performing models for each architecture. Details of the ablation studies and the parameter sweeps over model parameters can be found in the Appendix VI-C.

V. RESULTS

A. Dexterity of the *D’Manus*

We qualitatively demonstrate the dexterous capabilities of the *D’Manus* (Fig. 5) from interactions with everyday objects. We observe that the *D’Manus* is effective at grasping

and (in-hand as well as hand-arm) manipulation of day-to-day objects. Its abilities, however, are somewhat restricted for in-hand manipulation of small objects (e.g. counting coins on palm). This is in accordance with the dexterity and robustness trade-off we made and detailed in Sec. III-A.

B. Object Identification using Tactile Data

To validate the capability of the *D’Manus* to distinguish objects based on their texture and softness, we start with a simple object identification task. The goal of this task is to use learned discriminative models to quantify the differentiability of the tactile information obtained by the *D’Manus*. We pick a set of six objects and allow the *D’Manus* to interact with these objects. This data is used to train neural networks that can identify the object in contact purely from tactile information. We use this restrictive, controlled setting to ensure that models can only learn to differentiate using contact surface characteristics. We explicitly make this task agnostic to shape and size by using a set of six *identical* balls, each with a different outer covering – small bubble wrap, large bubble wrap, corrugated cardboard, silicone sponge, a combination of all these materials, and no covering material – as shown in Fig. 6. We collect 35 trajectories for each ball and use a 30-5 train-validation split.

We train classification models to learn to predict one of the six objects from tactile interaction data. These models are trained using standard cross-entropy loss minimization. Results for *Object Identification* can be found in Table II. We see that our networks are successfully able to distinguish between the six balls, thereby confirming the discriminability of the tactile data. Further, we note that the MLP and the RNN models are comparable in performance for this simple task. As we move to more difficult tasks in the following sections, we begin to see a greater discrepancy in performance.

Model type	Architecture Details ²	Validation Acc
<i>Object Identification</i>		
MLP	[256, 128, 64]	72.00%
RNN	LSTM(512*2) → [512]	71.24%
<i>Softness Classification</i>		
MLP	[256, 128, 64]	71.38%
RNN	LSTM(512*2) → [512]	76.17%
<i>Texture Classification: Vanilla</i>		
MLP	[512, 512, 512]	30.43%
RNN	LSTM(512*2) → [512]	30.67%
<i>Texture Classification: Joint Softness-Texture</i>		
MLP	[256, 128, 64]	32.85%
RNN	LSTM(512*2) → [512]	36.65%
<i>Texture Classification: Softness-Conditioned</i>		
MLP	[64, 64, 64]	48.85%
RNN	LSTM(512*2) → [256,128,64]	59.03%

TABLE II: Comparison of different neural architectures on the object identification, and softness and texture identification tasks

²We use ReLU activation between hidden layers. $[a, b, c]$ denotes 3 fully-connected layers of sizes a , b and c respectively. LSTM($k * N$) denotes N LSTM hidden layers of size k

C. Category-Level Softness and Texture Identification

Having verified the ability of the *D’Manus* to use contact characteristics to distinguish objects, we investigate its ability to learn tactile inference models that can generalize to unseen objects. To learn general identification models, we would need quantifiable descriptions of surface characteristics that can extend to unseen objects. We decide to use softness and texture as these descriptions and create a three-point scale to quantify softness – Hard, Medium, Soft – as well as texture – Smooth, Medium, Rough. We manually assign softness and texture labels to over 50 objects by consensus among the authors **before** starting the study. A few sample objects from each of these categories can be seen in Fig. 7. The goal is to learn softness and texture classification models and examine their generalizability to unseen objects. We use a set of 18 training objects and 9 validation objects for these tasks³. The corresponding datasets are created by collecting 15 trajectories of tactile interaction data for each of the training objects and 5 trajectories for each of the validation objects.

1) *Softness Classification*: We train two sets of classification models – the MLP and RNN models defined in Sec. IV-C – to predict softness categories. The performance of the best performing models in each set is presented in Table II. While our models are able to successfully distinguish between objects on the softness scale, we also note that the RNN performs better than the MLP. This increased margin of performance can be attributed to the LSTM’s ability to better capture temporal correlations between data and make better predictions as a result.

2) *Texture Classification*: Similarly, we train MLP and RNN models for texture classification. These *vanilla* models however, fail to generalize to the validation set. This failure can be attributed to the dependence of texture on object softness. Texture in this context refers to spatial discontinuities in the force profile felt by the interface in contact with the object. Gradation of texture therefore varies significantly with changes in softness. As a case in point, think about a neatly folded T-shirt – while this folded T-shirt can be said to have smooth texture, the same T-shirt clumped into a ball will have a number of folds that could make it feel highly textured. For a harder object, like the spiky ball in the bottom left corner of Fig. 7, the texture remains consistent due to its structural integrity. Further, the interaction force profile is spatially discontinuous to a larger extent than softer textured objects. Thus, object texture is difficult to quantify and analyze independently of softness properties.

To get around this problem, we perform an ablation study with two additional texture classification models – a *Joint Softness-Texture* prediction model that learns to jointly predict softness and texture and three individual *Softness-Conditioned* models corresponding to each of the softness categories. Each individual *Softness-Conditioned* model is trained on the subset of the training data corresponding to the softness category. We report the mean accuracy

³Details of all labelled objects can be found in the Appendix



Fig. 5: Illustration of the *D'Manus* grasping different objects

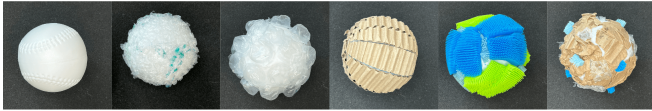


Fig. 6: **Material coverings for Object Identification Task:** Uncovered, small bubble wrap, large bubble wrap, corrugated cardboard, silicone sponge and combination of materials



Fig. 7: **Softness and Texture Categories:** Sample objects for the three-point scales defined in Sec. V-C

over these models in Table II, and note that the softness-conditioned models significantly outperform other models. This improvement in performance can be attributed to the disentanglement of softness and texture allowing the models to capture meaningful texture information.

As the *D'Manus* operates in unstructured environments where it interacts with objects of varying shapes and sizes, it is possible that different parts of the hand are in contact with different objects at any given time (Fig1). This would require prediction models corresponding to individual components of the hand to be good at independently identifying contact characteristics. To investigate this capability, we evaluate the performance of individual models learned on data from each component of the hand and present the results in Table III. The performance on the individual finger models is significantly lower than the palm as well as the full prediction model. This discrepancy can be explained by the fingers making and breaking contact in the course of the data

collection policy while the palm continues to stay in contact. This ability to effectively capture contact characteristics with individual components of the hand holds the *D'Manus* in good stead for operating in cluttered, unstructured human environments.

Component	Softness Accuracy	Texture Accuracy
Finger 1	56.27%	49.77%
Finger 2	48.48%	46.99%
Finger 3	59.59%	50.50%
Palm	74.31%	54.20%
All	76.17%	59.03%

TABLE III: Comparison of models trained using data from different components of the hand.

D. Tactile Bin Sorting

As our final experiment, we examine the capacity of our trained models to generalize to realistic environments and tasks. For this evaluation, we pick a cluttered bin sorting experiment. We attempt to pick objects from a cluttered bin and sort them according to softness and texture from tactile signals as a test of the generalizability of our learned models. We start with a cluttered bin containing a variety of objects as shown in Fig. 1. The robot samples a random location above the bin and reaches down into the bin. Once the magnitude of the ReSkin signal from the *D'Manus* exceeds a certain threshold, the hand stops moving and executes a grasp. If it successfully grasps an object, we predict the softness and texture of the grasped object. We then replace it with a new object and the process is continued. Over 20 successful grasps of different objects, our models achieve a prediction accuracy of 65% on both softness and texture prediction, confirming the ability of our models to extend to unseen tasks and environments in the real world.

VI. CONCLUSIONS AND LIMITATIONS

We present the *D'Manus* – a low-cost, 3D printable, prehensile robotic hand with multiple actuation modes, proprioceptive sensing abilities as well as ReSkin-based large-area tactile sensing. We demonstrate the dexterity of this platform by grasping a variety of objects. To exemplify the utility of the large-area sensing, we validate the discriminability of the tactile signal by learning models for object identification as well as category-level softness and texture identification. Further, we illustrate the transferability of learned tactile models to unstructured, real-world environments through a touch-based bin picking and sorting task.

Limitations: While we validate the tactile capabilities of the hand, we would like to fully evaluate the dexterous

capabilities of the hand by integrating tactile sensing into a dexterous policy learning setup in future work. In addition, we believe that unlocking the full potential of all-over tactile sensing requires the integration of other sensory modalities like vision and audio, allowing the robotic system richer sensory inputs to solve complex dexterous tasks. Finally, another limitation of this work is the lack of quantitative comparisons to other existing platforms due to the high resource cost involved in such a pursuit.

ACKNOWLEDGMENTS

The authors thank Vani Sundaram for her help with fixing ReSkin circuits, and all the members of FAIR Pittsburgh, AGI-Labs, and SML at CMU for their valuable inputs.

REFERENCES

- [1] L. Pinto and A. Gupta, “Supersizing self-supervision: Learning to grasp from 50k tries and 700 robot hours,” in *2016 IEEE international conference on robotics and automation (ICRA)*, pp. 3406–3413, IEEE, 2016.
- [2] S. Levine, P. Pastor, A. Krizhevsky, J. Ibarz, and D. Quillen, “Learning hand-eye coordination for robotic grasping with deep learning and large-scale data collection,” *The International journal of robotics research*, vol. 37, no. 4-5, pp. 421–436, 2018.
- [3] C. Bodnar, A. Li, K. Hausman, P. Pastor, and M. Kalakrishnan, “Quantile qt-opt for risk-aware vision-based robotic grasping,” in *Proceedings of Robotics: Science and Systems*, (Corvallis, Oregon, USA), July 2020.
- [4] A. Rajeswaran, V. Kumar, A. Gupta, G. Vezzani, J. Schulman, E. Todorov, and S. Levine, “Learning complex dexterous manipulation with deep reinforcement learning and demonstrations,” *arXiv preprint arXiv:1709.10087*, 2017.
- [5] T. Chen, J. Xu, and P. Agrawal, “A system for general in-hand object re-orientation,” in *Conference on Robot Learning*, pp. 297–307, PMLR, 2022.
- [6] P. Tuffield and H. Elias, “The shadow robot mimics human actions,” *Industrial Robot: An International Journal*, 2003.
- [7] M. Ahn, H. Zhu, K. Hartikainen, H. Ponte, A. Gupta, S. Levine, and V. Kumar, “Robel: Robotics benchmarks for learning with low-cost robots,” in *Conference on robot learning*, pp. 1300–1313, PMLR, 2020.
- [8] K. Chin, T. Hellebrekers, and C. Majidi, “Machine learning for soft robotic sensing and control,” *Advanced Intelligent Systems*, vol. 2, no. 6, p. 1900171, 2020.
- [9] O. M. Andrychowicz, B. Baker, M. Chociej, R. Jozefowicz, B. McGrew, J. Pachocki, A. Petron, M. Plappert, G. Powell, A. Ray, *et al.*, “Learning dexterous in-hand manipulation,” *The International Journal of Robotics Research*, vol. 39, no. 1, pp. 3–20, 2020.
- [10] R. L. Klatzky and S. J. Lederman, “Touch.,” 2013.
- [11] H. Yousef, M. Boukallel, and K. Althoefer, “Tactile sensing for dexterous in-hand manipulation in robotics—a review,” *Sensors and Actuators A: physical*, vol. 167, no. 2, pp. 171–187, 2011.
- [12] R. Bhirangi, T. Hellebrekers, C. Majidi, and A. Gupta, “Re-skin: versatile, replaceable, lasting tactile skins,” *arXiv preprint arXiv:2111.00071*, 2021.
- [13] T. Hellebrekers, O. Kroemer, and C. Majidi, “Soft magnetic skin for continuous deformation sensing,” *Advanced Intelligent Systems*, vol. 1, no. 4, p. 1900025, 2019.
- [14] M. Cherif and K. K. Gupta, “Planning quasi-static fingertip manipulations for reconfiguring objects,” *IEEE Transactions on Robotics and Automation*, vol. 15, no. 5, pp. 837–848, 1999.
- [15] A. Bicchi, “Hands for dexterous manipulation and robust grasping: A difficult road toward simplicity,” *IEEE Transactions on robotics and automation*, vol. 16, no. 6, pp. 652–662, 2000.
- [16] D. Rus, “Dexterous rotations of polyhedra,” in *Proceedings 1992 IEEE International Conference on Robotics and Automation*, pp. 2758–2759, IEEE Computer Society, 1992.
- [17] V. Kumar, A. Gupta, E. Todorov, and S. Levine, “Learning dexterous manipulation policies from experience and imitation,” *arXiv preprint arXiv:1611.05095*, 2016.
- [18] A. Nagabandi, K. Konolige, S. Levine, and V. Kumar, “Deep dynamics models for learning dexterous manipulation,” in *Conference on Robot Learning*, pp. 1101–1112, PMLR, 2020.
- [19] H. Zhu, A. Gupta, A. Rajeswaran, S. Levine, and V. Kumar, “Dexterous manipulation with deep reinforcement learning: Efficient, general, and low-cost,” in *2019 International Conference on Robotics and Automation (ICRA)*, pp. 3651–3657, IEEE, 2019.
- [20] M. Kopicki, R. Detry, M. Adjigble, R. Stolkin, A. Leonardis, and J. L. Wyatt, “One-shot learning and generation of dexterous grasps for novel objects,” *The International Journal of Robotics Research*, vol. 35, no. 8, pp. 959–976, 2016.
- [21] A. Zeng, P. Florence, J. Tompson, S. Welker, J. Chien, M. Attarian, T. Armstrong, I. Krasin, D. Duong, V. Sindhwani, *et al.*, “Transporter networks: Rearranging the visual world for robotic manipulation,” *arXiv preprint arXiv:2010.14406*, 2020.
- [22] H. Van Hoof, T. Hermans, G. Neumann, and J. Peters, “Learning robot in-hand manipulation with tactile features,” in *2015 IEEE-RAS 15th International Conference on Humanoid Robots (Humanoids)*, pp. 121–127, IEEE, 2015.

- [23] D. Gandhi, A. Gupta, and L. Pinto, "Swoosh! rattle! thump!—actions that sound," *arXiv preprint arXiv:2007.01851*, 2020.
- [24] S. Clarke, T. Rhodes, C. G. Atkeson, and O. Kroemer, "Learning audio feedback for estimating amount and flow of granular material," *Proceedings of Machine Learning Research*, vol. 87, 2018.
- [25] M. Du, O. Y. Lee, S. Nair, and C. Finn, "Play it by ear: Learning skills amidst occlusion through audio-visual imitation learning," *arXiv preprint arXiv:2205.14850*, 2022.
- [26] R. Calandra, A. Owens, D. Jayaraman, J. Lin, W. Yuan, J. Malik, E. H. Adelson, and S. Levine, "More than a feeling: Learning to grasp and regrasp using vision and touch," *IEEE Robotics and Automation Letters*, vol. 3, no. 4, pp. 3300–3307, 2018.
- [27] H. Van Hoof, N. Chen, M. Karl, P. van der Smagt, and J. Peters, "Stable reinforcement learning with autoencoders for tactile and visual data," in *2016 IEEE/RSJ international conference on intelligent robots and systems (IROS)*, pp. 3928–3934, IEEE, 2016.
- [28] M. T. Mason and J. K. Salisbury Jr, "Robot hands and the mechanics of manipulation," 1985.
- [29] G. A. Bekey, R. Tomovic, and I. Zeljkovic, "Control architecture for the belgrade/usc hand," in *Dextrous robot hands*, pp. 136–149, Springer, 1990.
- [30] S. Jacobsen, E. Iversen, D. Knutti, R. Johnson, and K. Biggers, "Design of the utah/mit dextrous hand," in *Proceedings. 1986 IEEE International Conference on Robotics and Automation*, vol. 3, pp. 1520–1532, IEEE, 1986.
- [31] T. Iberall, "Human prehension and dextrous robot hands," *The International Journal of Robotics Research*, vol. 16, no. 3, pp. 285–299, 1997.
- [32] P. J. Kyberd and P. H. Chappell, "The southampton hand: an intelligent myoelectric prosthesis," *Journal of Rehabilitation Research and Development*, vol. 31, no. 4, p. 326, 1994.
- [33] R. Tomovic and G. Boni, "An adaptive artificial hand," *IRE Transactions on Automatic Control*, vol. 7, no. 3, pp. 3–10, 1962.
- [34] C. Pfeiffer, K. DeLaurentis, and C. Mavroidis, "Shape memory alloy actuated robot prostheses: initial experiments," in *Proceedings 1999 IEEE International Conference on Robotics and Automation (Cat. No. 99CH36288C)*, vol. 3, pp. 2385–2391, IEEE, 1999.
- [35] C. Piazza, G. Grioli, M. Catalano, and A. Bicchi, "A century of robotic hands," *Annual Review of Control, Robotics, and Autonomous Systems*, vol. 2, pp. 1–32, 2019.
- [36] M. Wüthrich, F. Widmaier, F. Grimmering, J. Akpo, S. Joshi, V. Agrawal, B. Hammoud, M. Khadiv, M. Bogdanovic, V. Berenz, et al., "Trifinger: An open-source robot for learning dexterity," *arXiv preprint arXiv:2008.03596*, 2020.
- [37] N. Wettels, V. J. Santos, R. S. Johansson, and G. E. Loeb, "Biomimetic tactile sensor array," *Advanced Robotics*, vol. 22, pp. 829–849, 2008.
- [38] K. Hosoda, Y. Tada, and M. Asada, "Anthropomorphic robotic soft fingertip with randomly distributed receptors," *Robotics and Autonomous Systems*, vol. 54, no. 2, pp. 104–109, 2006.
- [39] D. V. Dao, S. Sugiyama, S. Hirai, et al., "Analysis of sliding of a soft fingertip embedded with a novel micro force/moment sensor: Simulation, experiment, and application," in *2009 IEEE International Conference on Robotics and Automation*, pp. 889–894, IEEE, 2009.
- [40] A. Schmitz, M. Maggiali, M. Randazzo, L. Natale, and G. Metta, "A prototype fingertip with high spatial resolution pressure sensing for the robot icub," in *Humanoids 2008-8th IEEE-RAS International Conference on Humanoid Robots*, pp. 423–428, IEEE, 2008.
- [41] F. Veiga, B. B. Edin, and J. Peters, "In-hand object stabilization by independent finger control," *arXiv preprint arXiv:1806.05031*, 2018.
- [42] T. P. Tomo, A. Schmitz, W. K. Wong, H. Kristanto, S. Somlor, J. Hwang, L. Jamone, and S. Sugano, "Covering a robot fingertip with uskin: A soft electronic skin with distributed 3-axis force sensitive elements for robot hands," *IEEE Robotics and Automation Letters*, vol. 3, no. 1, pp. 124–131, 2017.
- [43] B. Sundaralingam, A. S. Lambert, A. Handa, B. Boots, T. Hermans, S. Birchfield, N. Ratliff, and D. Fox, "Robust learning of tactile force estimation through robot interaction," in *2019 International Conference on Robotics and Automation (ICRA)*, pp. 9035–9042, IEEE, 2019.
- [44] J. M. Elliott and K. Connolly, "A classification of manipulative hand movements," *Developmental Medicine & Child Neurology*, vol. 26, no. 3, pp. 283–296, 1984.
- [45] K. Pont, M. Wallen, and A. Bundy, "Conceptualising a modified system for classification of in-hand manipulation," *Australian occupational therapy journal*, vol. 56, no. 1, pp. 2–15, 2009.
- [46] B. Shih, D. Shah, J. Li, T. G. Thuruthel, Y.-L. Park, F. Iida, Z. Bao, R. Kramer-Bottiglio, and M. T. Tolley, "Electronic skins and machine learning for intelligent soft robots," *Science Robotics*, vol. 5, no. 41, p. eaaz9239, 2020.
- [47] G. Cannata, M. Maggiali, G. Metta, and G. Sandini, "An embedded artificial skin for humanoid robots," in *2008 IEEE International conference on multisensor fusion and integration for intelligent systems*, pp. 434–438, IEEE, 2008.
- [48] T. Hoshi and H. Shinoda, "A large area robot skin based on cell-bridge system," in *SENSORS, 2006 IEEE*, pp. 827–830, IEEE, 2006.
- [49] W. Yuan, S. Dong, and E. H. Adelson, "Gelsight: High-resolution robot tactile sensors for estimating geometry and force," *Sensors*, vol. 17, no. 12, p. 2762, 2017.
- [50] M. Lambeta, P.-W. Chou, S. Tian, B. Yang, B. Maloon, V. R. Most, D. Stroud, R. Santos, A. Byagowi, G. Kammerer, et al., "Digit: A novel design for a low-cost compact high-resolution tactile sensor with application to in-hand manipulation," *IEEE Robotics and Automation Letters*, vol. 5, no. 3, pp. 3838–3845, 2020.
- [51] S. Sundaram, P. Kellnhofer, Y. Li, J.-Y. Zhu, A. Torralba, and W. Matusik, "Learning the signatures of the human grasp using a scalable tactile glove," *Nature*, vol. 569, no. 7758, pp. 698–702, 2019.
- [52] E. Dean-Leon, J. R. Guadarrama-Olvera, F. Bergner, and G. Cheng, "Whole-body active compliance control for humanoid robots with robot skin," in *2019 International Conference on Robotics and Automation (ICRA)*, pp. 5404–5410, IEEE, 2019.
- [53] P. Mittendorf, E. Yoshida, and G. Cheng, "Realizing whole-body tactile interactions with a self-organizing, multi-modal artificial skin on a humanoid robot," *Advanced Robotics*, vol. 29, no. 1, pp. 51–67, 2015.
- [54] Y. Lin, A. S. Wang, G. Sutanto, A. Rai, and F. Meier, "Polymetis." <https://facebookresearch.github.io/fairo/polymetis/>, 2021.

APPENDIX

A. Classification Datasets

1) *Object Identification with Tactile Data*: Our set of objects for small-scale object classification consists of six identical plastic balls of 3.5 inch diameter.

2) *Category-Level Softness and Texture Identification*: We used a wide variety of household objects to collect data for category-level softness and texture identification experiments so as to enable and demonstrate the generalization capability of the D’Manus. Figures 9, 10 and 11 shows the training, validation and test sets used for these experiments.

B. Data Collection and Inference

All training and validation data is collected using the data collection setup described in Sec. IV-B. Data is collected at a frequency of 30 Hz and we collect a baseline measurement before the motor babble policy is executed. To do this, we place the object on the hand and collect 100 sensor measurements, which are then averaged to obtain the baseline measurement. Training and inference works by using baseline-subtracted data

When the models are deployed for bin picking, we use a similar approach to baseline measurement. The robot samples a random location above the bin and moves to this point. We collect 100 sensor measurements and average them to obtain a baseline measurement. The robot then descends and attempts a grasp based on a simple heuristic policy – the grasp is executed if the norm of the ReSkin data exceeds a threshold. If the grasp succeeds, the trained models are used to infer softness and texture labels from baseline-subtracted data.

The D’Manus weighs 1.5 kilograms (with Reskin sensing). We use Franka Emika robot arm for all our experiments. Figure 8 outlines the gravity compensation parameters we used. The coordinate frame for these parameters was chosen such that the positive z-axis is normal and pointing outwards from the surface of the palm. The positive x-axis bisects the palm and points from the base of the hand towards the index and little fingers.

C. Ablations and Parameter Sweeps

To build a better understanding of the best ways to process ReSkin data, we run a number of ablations and hyperparameter sweeps.

1) *Sweep over Frequency*: We test multiple sampling frequencies for the object identification task and create three datasets with sampling frequencies of 10, 20 and 30 Hz. We then train MLP as well as RNN models described in Sec. V, sweeping over different parameters of the respective models. We find that the performance of the MLP models does not vary significantly as the sampling frequency is varied. The performance of the RNN model, however, is seen to improve significantly with higher sampling frequencies as can be seen from Table IV. Due to the significant gain in performance of the RNN and the agnostic nature of the MLP, we stick to a frequency of 30 Hz in subsequent experiments.

Mass

1.8 kg

Flange to Center of Mass of Load Vector

0.065 0.02 0.05 m

Inertia Tensor

0.005 0 0

0 0.0062 0 kg × m².

0 0 0.0074

Transformation Matrix from Flange to End-Effector

0.7071 0.7071 0 0

-0.7071 0.7071 0 0

0 0 1 0

0 0 0 1

Fig. 8: Mass and Inertia matrices for gravity compensation

Frequency	RNN Validation Accuracy
10 Hz	87.04%
20 Hz	79.62%
30 Hz	68.52%

TABLE IV: RNN accuracy over different data collection frequencies for the object identification task

2) *Sweep over Neural Architecture parameters*: All the results presented in Sec. V correspond to the best performing parameters for the MLP as well as the RNNs. For the MLP we sweep over the number of layers, layer size, the number of stacked frames(`stack-size`) and the number of frames skipped between them(`frame-skip`) in the input to the network. Table V outlines the range of hyperparameters swept over. For the MLP, we found that a stack size of 2 worked best across tasks and was generally agnostic to the number of frames skipped between stack elements.

Hyperparameter	Sweep Range
MLP	
stack-size	[2, 5, 8, 11]
frame-skip	[2, 5, 8, 11]
number of layers	[2, 3, 4]
layer sizes	[64, 128, 256, 512, 1024]
RNN	
LSTM: number of layers	[2, 3, 4]
LSTM: layer size	[128, 256, 512, 1024]
fully-connected: number of layers	[1, 2, 3]
fully-connected: layer size	[64, 128, 256, 512]

TABLE V: Parameter ranges for hyperparameter sweeps

Training Data

	Hard			Medium			Soft		
Smooth									
Medium									
Rough									

Fig. 9: Training Dataset

Validation Data

	Hard	Medium	Soft
Smooth			
Medium			
Rough			

Fig. 10: Validation Dataset

Test Data

	Hard			Medium			Soft		
Smooth									
									
Medium									
Rough									

Fig. 11: Test Dataset